

Mon. Not. R. Astron. Soc. **000**, 1–?? (2007) Printed 27 October 2013 (MN  $\LaTeX$  style file v2.2)

# UV Bright Globular Clusters in M87: More Evidence for Super-helium-rich Stellar Populations?

S. Kaviraj<sup>1</sup>, S. T. Sohn<sup>2,3</sup>, R. W. O’Connell<sup>3</sup>, S. -J. Yoon<sup>4</sup>, Y. W. Lee<sup>4</sup> and S. K. Yi<sup>4\*</sup><sup>1</sup> *Department of Physics, University of Oxford, Keble Road, Oxford OX1 3RH, UK*<sup>2</sup> *Korea Astronomy and Space Science Institute, 61-1 Hwaam-Dong, Yuseong-Gu, Daejeon 305348, Korea*<sup>3</sup> *University of Virginia, Department of Astronomy, Charlottesville, VA 22904, USA*<sup>4</sup> *Yonsei University, Center for Space Astrophysics, Seoul 120749, Korea*

Accepted in MNRAS: 27 October 2013

## ABSTRACT

We study the *UV* and optical properties of 38 massive globular clusters (GCs) in the Virgo elliptical, M87, imaged using the *STIS* and *WFPC2* instruments onboard the *Hubble Space Telescope*. The majority of these GCs appear extremely bright in the far-ultraviolet (*FUV*) - roughly a magnitude brighter than their Galactic counterparts with similar metallicities. The observed *FUV* flux is several times larger than predictions of canonical old stellar population models. These canonical models, which assume a fiducial helium enrichment parameter,  $\Delta Y/\Delta Z = 2$ , are able to reproduce the observed *FUV* fluxes only if ages  $\sim 3\text{--}5$  Gyr larger than the “WMAP age” of the Universe are invoked, although the same models fit the *UV* photometry of Galactic and M31 GCs for ages less than the “WMAP age”. A similar discrepancy ( $\sim 3$  Gyr) is found between the mass-weighted and *UV*-luminosity weighted ages of the massive Galactic GC  $\omega$  Cen, whose colour-magnitude diagram (including peculiar features on its well-populated horizontal branch) can be accurately reproduced by invoking a small super-He-rich ( $\Delta Y/\Delta Z \gtrsim 90$ ) stellar component. By comparison to  $\omega$  Cen, we propose that the majority of M87 GCs in our sample contain strong signatures of similarly minor super-He-rich sub-components. This hypothesis is supported by simulations which suggest that, based on the *UV* detection limit of this survey, the number of GCs detected is several times of the prediction from canonical models. Although we cannot prove or disprove the extreme helium scenario at the moment, we show that the same phenomenon that causes the extended horizontal branch of  $\omega$  Cen explains

the UV brightness of our sample. If this is indeed due to the extreme helium, this study would be the first to find its signatures in extragalactic objects.

**Key words:** galaxies: elliptical and lenticular, cD – galaxies: evolution – galaxies: formation – galaxies: fundamental parameters – globular clusters: general

## 1 INTRODUCTION

Recent observations of the stellar population of the largest Galactic globular cluster (GC),  $\omega$  Cen, have revealed a double main sequence (MS), with a disjoint sub-population of bluer and fainter MS stars which is separated from a majority population of redder and brighter MS stars (e.g. Bedin et al. 2004). In addition,  $\omega$  Cen harbours a substantial population of extended horizontal branch (EHB) stars, which are hotter and distinct from the primary population of normal horizontal branch (HB) stars (Whitney et al. 1994; Ferraro et al. 2004; Sollima et al. 2005, 2006). Theoretical analysis has indicated that the double main sequence could be a result of a large spread in helium (He) abundances within the cluster (Norris 2004) - this is supported by spectroscopic measurements of metal abundances of MS stars in  $\omega$  Cen (Piotto et al. 2005). More recently, Lee et al. (2005) have shown that a large variation in the He abundance in  $\omega$  Cen can not only reproduce the double MS, but also accounts naturally for the ‘anomalous’ population of hot extended HB stars in this cluster<sup>1</sup>. Their best simulation of  $\omega$  Cen requires the He enrichment ( $\Delta Y/\Delta Z$ ) parameter, for a minority population of stars, to be in excess of 90 - for comparison  $\Delta Y/\Delta Z \sim 2$  on galactic scales (e.g., Peimbert et al. 2001). Although such high values of helium enrichment are difficult to reproduce theoretically (e.g., Bekki & Norris 2006; Choi & Yi 2007; Karakas et al. 2006), similar super-He-rich sub-populations are also capable of reproducing the peculiar HB morphology of another Galactic GC, NGC 2808 (D’Antona & Caloi 2004; Bedin et al. 2000; Lee et al. 2005; D’Antona et al. 2005). A similar phenomenon may be responsible for the unusually-blue HB morphology of NGC 6338, and NGC 6441 for their metallicities (e.g., Sweigart & Catelan 1998; Caloi & D’Antona 2006).

Helium-rich populations are thought to have a significantly higher number of hot, evolved HB stars and thus show enhanced *UV* fluxes (and hence bluer integrated *UV* colours)

\* Send offprint request to yi@yonsei.ac.kr

<sup>1</sup> Note that the evidence for He enrichment in  $\omega$  Cen does not come from direct observations of He spectral lines but is inferred from the HB morphology and direct determinations of metallicity.

than helium-poor counterparts of the same age (e.g. Dorman et al. 1995; Yi et al. 1997, 1998, 1999). Using models with standard He enrichment ( $\Delta Y/\Delta Z \sim 2$ ) to derive ages from such integrated *UV* colours would therefore lead to those ages being *overestimated*, since populations with standard He enrichment take *longer* to output the same level of *UV* flux as those with a super-He-rich sub-component. Reversing this argument implies that the detection of GCs that are too blue to be produced by old populations with standard He enrichment, might indicate the presence of anomalously high He concentrations in the stellar populations within these clusters. In this paper we present a plausibility argument for the presence of just such a population of GCs in the elliptical galaxy M87. The motivation for this work stems from the recent *UV* study of M87 globular clusters (see Sohn et al. 2006). We find that (a) the *FUV* detection rate of M87 globular clusters in this study is *significantly* larger than can be expected from simulations of a standard old stellar population that has a He enrichment value of  $\sim 2$  and that (b) the majority of globular clusters which *are* detected have derived (*FUV*-weighted) ages which are far in excess of the presently-accepted age of the Universe. In this study, we adopt the most recent estimate from the WMAP data as the “physical” age of the Universe (Spergel et al. 2006). Since the stellar models used to perform the GC age estimation are well-calibrated to Galactic GCs, and produce physical ages ( $\lesssim 13$  Gyr) for old GCs in M31, we argue that both pieces of evidence are consistent with the existence of super-He-rich populations in the GC system of M87, and that indeed it may be the *FUV*-enhanced ‘super-helium-enriched’ tail of the GC distribution which has been sampled by this study, given that the *FUV* detection rate is far higher than that expected for a normal population of HB stars.

## 2 PARAMETER ESTIMATION: AGE AND METALLICITY OF M87 GCS

We begin by combining *HST/STIS* broad-band *FUV* and *NUV* photometry from Sohn et al. (2006) with *HST/WFPC2* optical photometry from Jordán et al. (2002) in the *F336w*, *F410m*, *F467m* and *F547m* filters and photometry in the *V* and *I* filters from Kundu et al. (1999), to simultaneously estimate the ages and metallicities of 38 GCs in M87. GC star formation histories (SFHs) can be adequately parametrised by (dustless) simple stellar populations (SSPs) of a given age and metallicity alone, and our parameter estimation employs a finely-interpolated grid of SSPs using the Yi-Yoon stellar models (see e.g. Yi 2003). The parameter estimation proceeds as follows:

For a vector  $\mathbf{X}$  denoting parameters in the model, and a vector  $D$  denoting the measured observables (data),

$$\text{prob}(\mathbf{X}|D) \propto \text{prob}(D|\mathbf{X}) \times \text{prob}(\mathbf{X}), \quad (1)$$

where  $\text{prob}(\mathbf{X}|D)$  is the probability of the model given the data (which is the object of interest),  $\text{prob}(D|\mathbf{X})$  is the probability of the data given the model and  $\text{prob}(\mathbf{X})$  is the prior probability distribution of the model parameters

If we assume a uniform prior in our model parameters i.e.

$$\text{prob}(\mathbf{X}) = \text{constant}, \quad (2)$$

we have

$$\text{prob}(\mathbf{X}|D) \propto \text{prob}(D|\mathbf{X}). \quad (3)$$

Assuming Gaussian errors on the measured quantities gives

$$\text{prob}(D|\mathbf{X}) \propto \exp(-\chi^2/2), \quad (4)$$

where  $\exp(-\chi^2/2)$  is the likelihood function and  $\chi^2$  is the sum of the normalised residuals between the model-predicted observables  $M_k$  and the observed values  $D_k$

$$\chi^2 = \sum_{k=1}^N \left( \frac{M_k - D_k}{\sigma_k} \right)^2, \quad (5)$$

and  $\sigma_k$  is the error in the residual  $M_k - D_k$ .  $\text{prob}(\mathbf{X}|D)$  is a *joint* PDF, dependent on all the model parameters. To isolate the effect of a single parameter  $X_1$  in, for example, a two parameter model ( $\text{prob}(\mathbf{X}|D) \equiv \text{prob}(X_1, X_2|D)$ ) we can integrate out the effect of  $X_2$  to obtain the *marginalised* PDF for  $X_1$ :

$$\text{prob}(X_1|D) = \int_0^\infty \text{prob}(X_1, X_2|D) dX_2. \quad (6)$$

In our analysis, the parameters  $\mathbf{X}$  in the model are the age ( $t$ ) and metallicity ( $Z$ ) of the SSP in question, and the observables are colours constructed from *UV* and optical photometry. We choose a uniform prior in  $t$ , in the range 1 to 18 Gyr. For the metallicity  $Z$ , we use a uniform prior in the range  $-2.3$  to  $0.7$  dex, which are essentially the metallicity limits of the stellar models. For each GC analysed, we marginalise the age and metallicity parameters, take the *peak* ( $x_0$ ) of the marginal PDF  $P(x)$  as the best estimate and *define* one-sigma limits  $x_+$  and  $x_-$  as follows:

$$\int_{x_0}^{x_+} P(x) dx = 0.34 \int_{x_0}^{\infty} P(x) dx \quad (7)$$

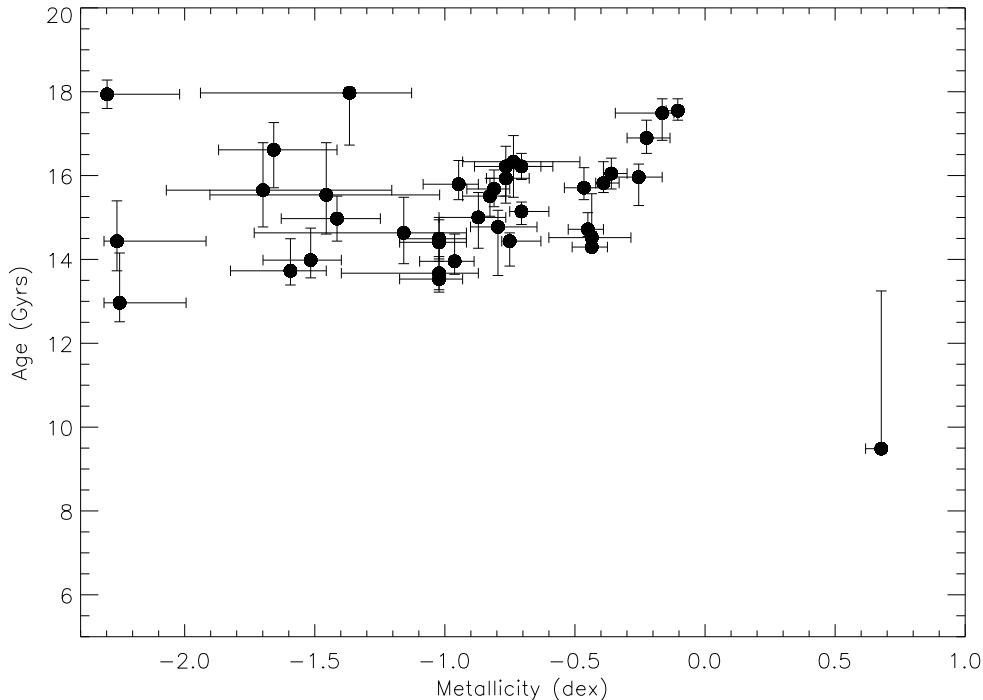


**Figure 1.** Age and metallicity estimates for M87 GCs using *UV* and optical photometry (8 bands in total).

$$\int_{x_-}^{x_0} P(x)dx = 0.34 \int_{-\infty}^{x_0} P(x)dx \quad (8)$$

We define the *uncertainty* in the estimate of a parameter as  $(x_+ + x_-)$  i.e. the total extent of the one-sigma limits in parameter space.

In Figure 1 we show the estimates of age and metallicity for each GC, derived using this procedure from a set of stellar models which has the fiducial value of He enrichment ( $\Delta Y/\Delta Z = 2$ ). We do not find a clear hint for a substantial difference in age between the metal-poor and metal-rich GCs, in agreement with the result of Jordán et al. (2002).

Figure 2 shows the marginalised probability density function (PDF) for age and metallicity for all M87 GCs used in this study. The metallicity PDF appears multi-modal. Applying the KMM test for *bimodality* yields two peaks: a metal-poor peak at  $-1.33$  dex and a metal-rich peak at  $-0.25$  dex. These values agree reasonably well with Jordán et al. (2002), who report values of  $-1.58$  dex and  $-0.30$  dex and Kundu et al. (1999), who find values of  $-1.41$  dex and  $-0.23$  dex. The KMM test accepts bimodality at the 98 percent confidence level and trimodality at  $> 99.9$  percent confidence. However, we note that the trimodality, in particular, is weak and that the small size of the sample, coupled with its *UV*-selected nature makes it unreliable to extrapolate this metallicity PDF to the entire M87 GC population!

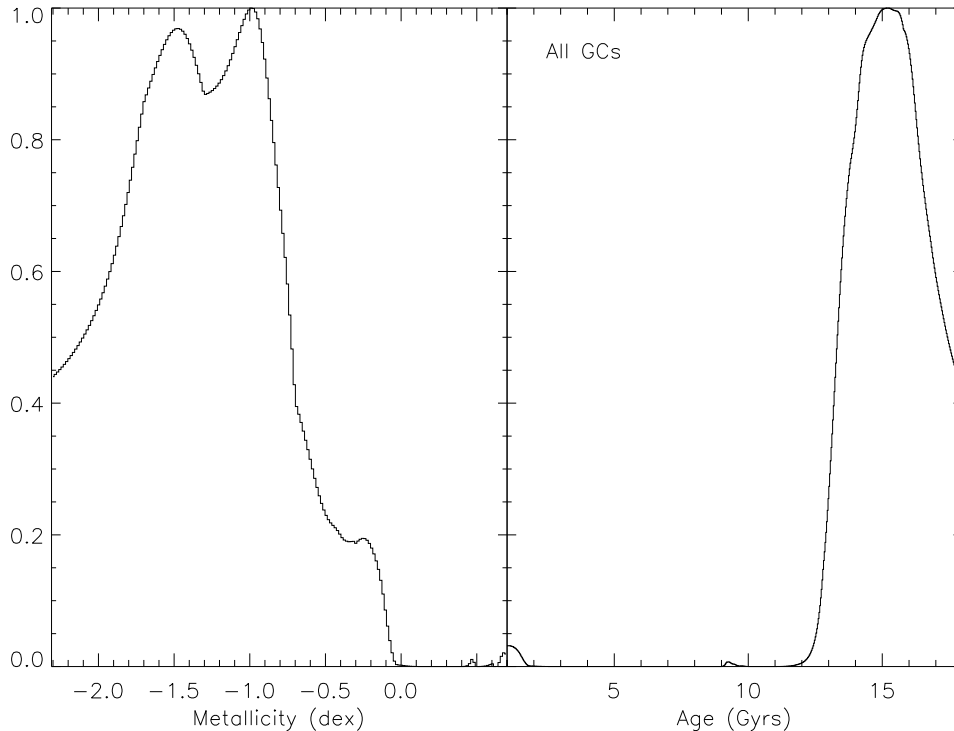


**Figure 2.** Marginalised probability density functions for age and metallicity for all M87 GCs used in this study.

Since the metallicity estimation in this study is derived from 8 photometric filters instead of one single colour index, it is plausible that we are better able to resolve the metallicity of the population and, in particular, the bimodality of the metal-poor peak, which may not be obvious when using a single optical colour such as  $V - I$ . We cannot, however, estimate the *proportion* of each subpopulation from this data, because the GCs represent a *FUV selected sample* and are therefore unrepresentative of its parent population.

### 3 THE DERIVED AGES OF M87 GLOBULAR CLUSTERS

The ages derived in the last section, using the fiducial stellar models, range 14–18 Gyr, unphysically large given current estimates of the age of the universe. The technical reason for this apparent ‘overestimate’ of the age is that the M87 photometry largely lies *outside* the model colour-colour grids which cover the age of the universe ( $t \sim 14$  Gyr). We illustrate this by showing a model ( $FUV - V$ ) vs. ( $V - I$ ) grid in Figure 3. While the Milky Way GC data (open triangles) are reproduced by the grid, most of the M87 data (filled circles) lie outside the age range 1–14 Gyr for the generally-accepted metallicity range,  $[m/H] \lesssim +0.2$  (Cohen et al. 1998).

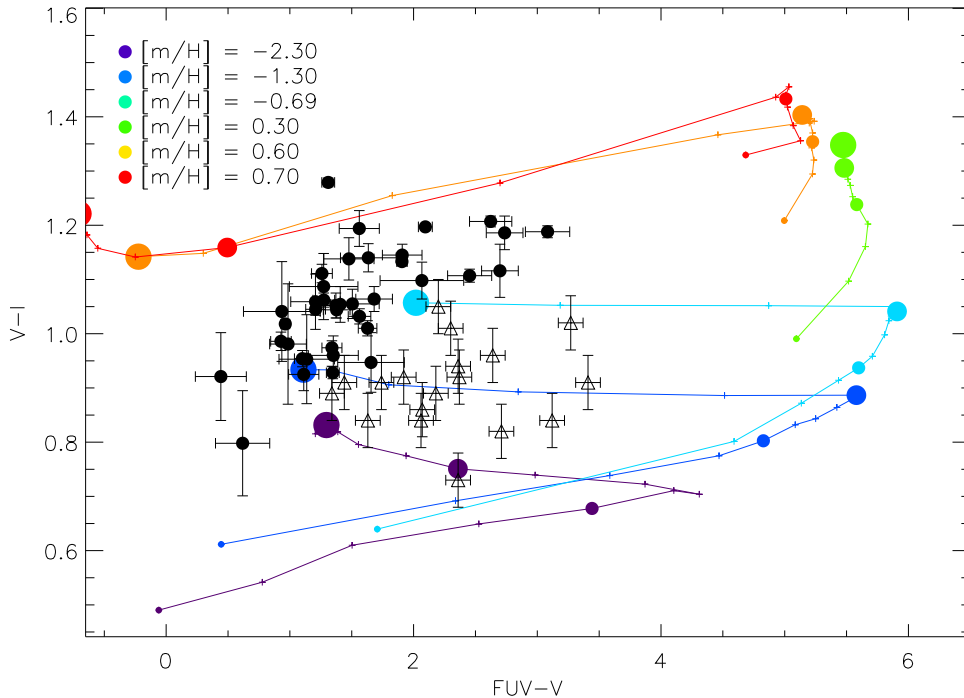


**Figure 3.** Model ( $FUV - V$ ) vs. ( $V - I$ ) grid for a range of metallicities and ages, generated from stellar models with the fiducial value of He enrichment ( $\Delta Y / \Delta Z = 2$ ). The lowest age plotted is 1 Gyr and the largest age plotted is 15 Gyr. Ages 1, 5, 10 and 15 Gyr are shown using filled circles of increasing sizes. The GC data of M87 (filled circles) and Milky Way (open triangles) with errors are overplotted. It is apparent that the M87 photometry lies *outside* the age range 1-14 Gyr for all metallicities.

It is important to note that the ages derived for the M87 GCs in the previous section are essentially *FUV luminosity-weighted ages*. For comparison, we now seek an estimate of the age of the M87 GC population which *does not* rely on their *FUV* flux. We note that Cohen et al. (1998) have previously derived ages of M87 GCs (as a function of metallicity) using the Worthey (1994) models. We repeat their analysis, using their measurements of the Lick indices of M87 GCs (see their Table 1 for the specific indices used), but this time using the Bruzual & Charlot (2003, BC2003 hereafter) stellar models, which are more up to date. Using the BC2003 models, our Lick index-based age estimates on Cohen et al.’s M87 GCs are roughly 10–11 Gyr, which is somewhat lower than those of Cohen et al. (1998). Figure 4 shows the same information as Figure 1, with the ages determined from the Lick indices overplotted using open triangles. Lee et al. (2000) have previously noted that a population with a hot HB would appear younger in Lick indices by  $\sim 2$ –3 Gyr due to a significant contribution from the HB stars to the *B*-band flux. Even considering this effect, the Lick index ages are still 2–4 Gyr younger than the *UV*-derived ages.

We note here that the Cohen et al. (1998) sample does not overlap with the Sohn et al.

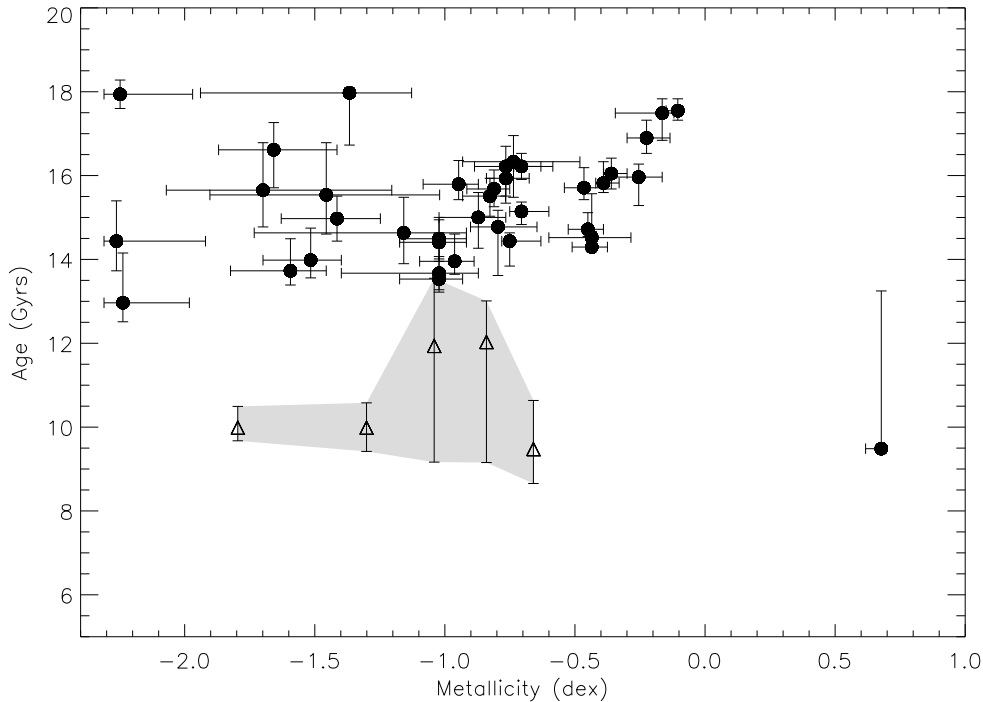


**Figure 4.** Same as Figure 1 but with the ages of M87 GCs (studied by Cohen et al. (1998)) determined from Lick absorption line indices and their uncertainties (open triangles with error bars and grey shaded region) added. See Table 1 of Cohen et al. (1998) for the Lick indices used in this age determination.

(2006) sample of GCs. Although we would ideally like to determine the ‘spectroscopic’ ages of the Sohn et al. GCs, no absorption line data exists for this sample and therefore we are not able to extract ages and metallicities for these objects independent of their *UV*-optical colours. However, if we now assume that (a) the Cohen et al. (1998) sample is representative of the *parent* M87 GC population and (b) the age derivation from Lick indices is closer to the *true* age of the M87 GC population than that derived from the *UV* photometry, then we find a  $\sim 2 - 3$  Gyr discrepancy between the the *FUV* luminosity-weighted mean age of M87 GCs in this sample and the ‘true’ age of the parent population. The discrepancy is driven by an enhancement of the *FUV* flux in these clusters beyond that expected from normal HB stars.

#### 4 *FUV* ENHANCEMENT IN M87 GCS: SUPER-HE-RICH STARS?

Lee et al. (2005) have recently suggested that a small super-He-rich stellar component reproduces both the peculiar features of the main sequence and the anomalous EHB population (which is hotter and emits significantly more *FUV* flux than normal HB stars) in  $\omega$  Cen.



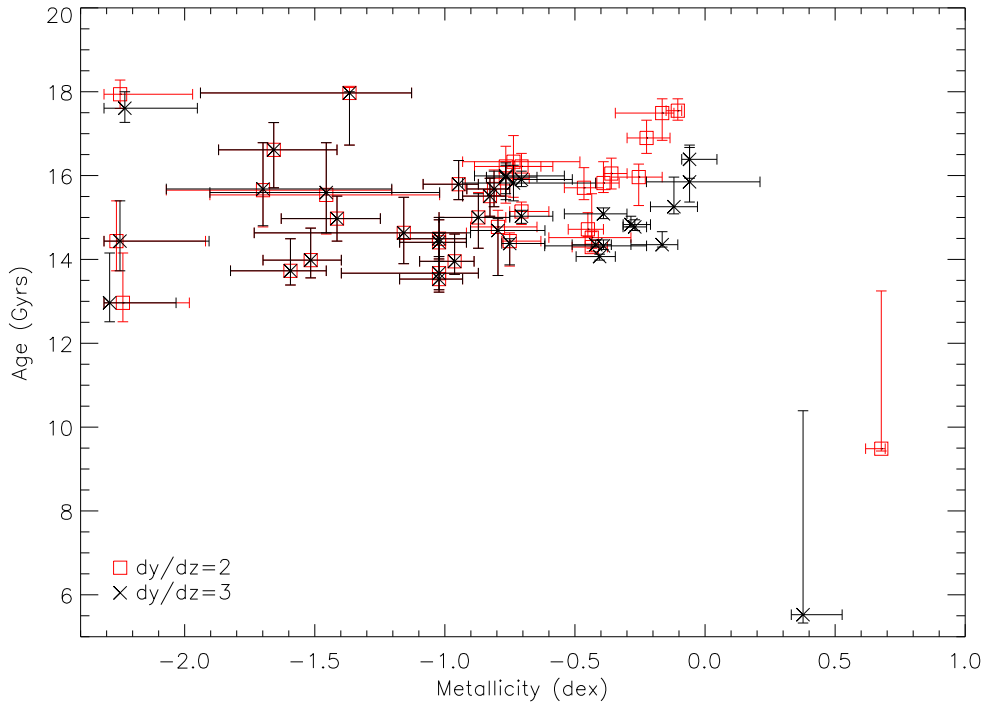


**Figure 5.** Comparison between age and metallicity derivations using the fiducial ( $\Delta Y/\Delta Z = 2$ , open red squares) and helium-enhanced ( $\Delta Y/\Delta Z = 3$ , black crosses) stellar models.

In this section, we explore the plausibility of a similar mechanism being responsible for the enhanced *FUV* flux seen in M87 GCs.

In order to explore the effect of enhanced He enrichment on the age derivation of the M87 GCs, we repeat the parameter estimation of Section 2 but replace the fiducial stellar model used previously ( $\Delta Y/\Delta Z = 2$ ) with a modestly helium-enhanced model where  $\Delta Y/\Delta Z = 3$ .

In Figure 5 we compare the age and metallicity derivations using the fiducial (open squares) and helium-enhanced (crosses) stellar models. We find that GCs which have best-fit metallicities higher than -1.0 dex show a *lower* best-fit age with the helium-enhanced model than the fiducial model. The use of an helium-enhanced model moves the *FUV* luminosity-weighted ages of the GCs closer to their ‘true’ ages, since He-rich stars are hotter and thus brighter in the *UV* than their He-poor counterparts for the same age and mass. Nevertheless, the modest helium-enrichment employed in the  $\Delta Y/\Delta Z = 3$  model does not lower the estimated ages sufficiently to achieve agreement with the spectroscopic ages.

The He enrichment ( $\Delta Y/\Delta Z > 90$ ), for a sub-population of stars, adopted in Lee et al. (2005) is significantly more extreme. To explore whether such extreme He enrichment could be present in the M87 GCs, we compare the *FUV* luminosity-weighted age of  $\omega$  Cen with its *probable* true age. To compute the true age of  $\omega$  Cen, we calculate the *mass-weighted* age

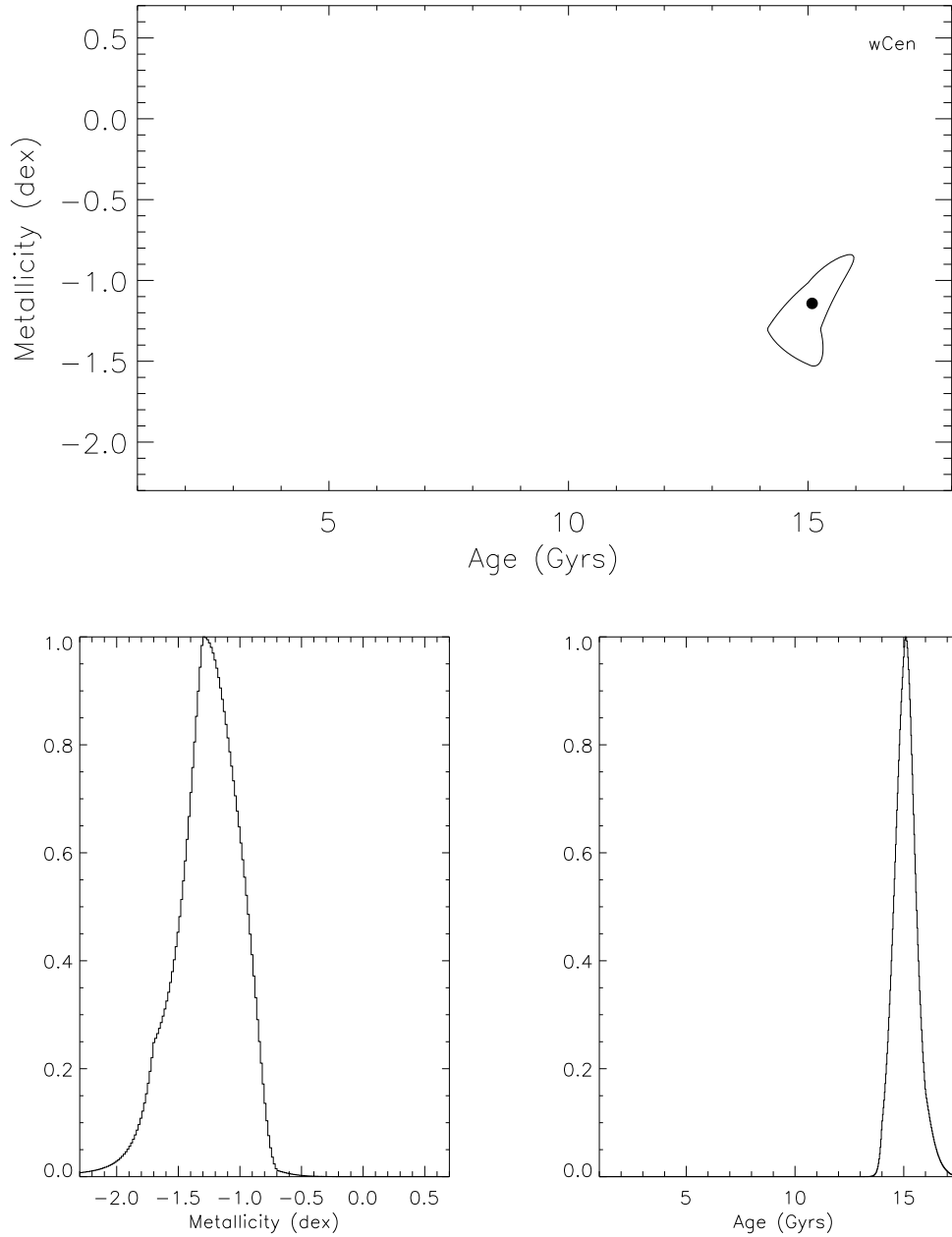


**Figure 6.** TOP PANEL: Best-fit age and metallicity estimate for  $\omega$  Cen and one-sigma contour. BOTTOM LEFT: Marginalised metallicity probability density function for  $\omega$  Cen. BOTTOM RIGHT: Marginalised age probability density function for  $\omega$  Cen.

of the best model of Lee et al. (2005), which accurately reproduces the observed CMD of  $\omega$  Cen (see Table 1 in their paper). This mass-weighted age is  $\sim 12$  Gyr. We then compute the *FUV* luminosity-weighted age for this GC, using its  $(15 - V)_0$ ,  $(25 - V)_0$  and  $(V - I)_0$  colours, taken from Dorman et al. (1995), and by performing the parameter estimation with the fiducial  $\Delta Y/\Delta Z = 2$  stellar model.

As Figure 6 indicates, the best-fit metallicity for  $\omega$  Cen is around  $-1.3 \pm 0.21$  dex (for

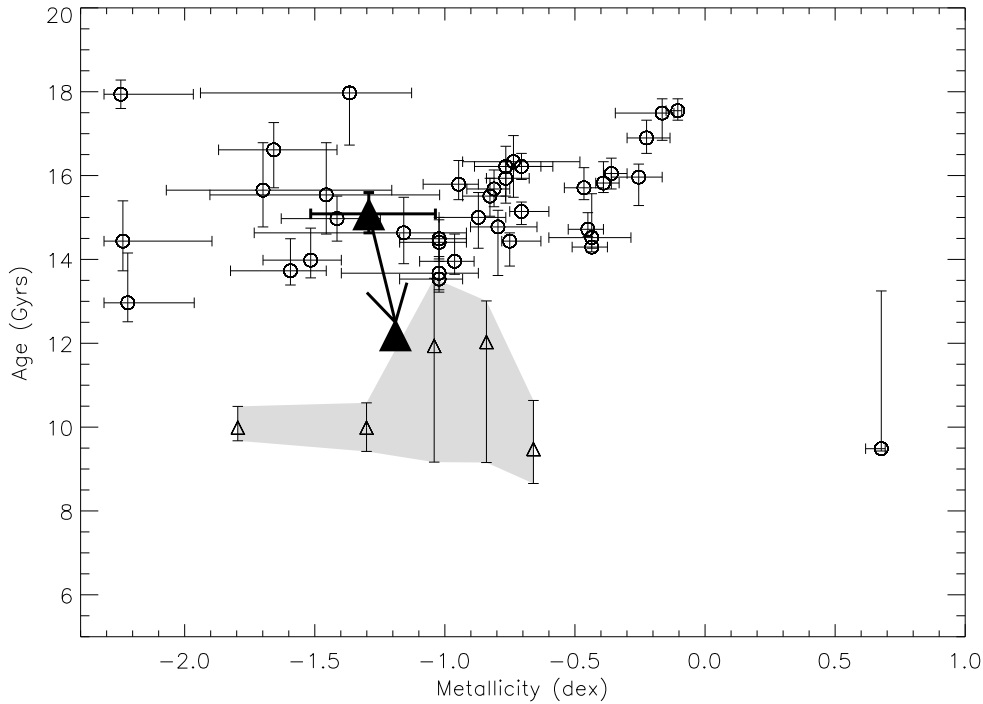


**Figure 7.** Age and metallicity estimates for M87 GCs, derived using *UV* and optical photometry (black circles with error bars). Ages of M87 GCs studied by Cohen et al. (1998), determined from Lick indices, are shown using the open triangles and grey shaded region. The *FUV* luminosity-weighted age (15.1 Gyr) and mass-weighted age ( $\sim 12$  Gyr) of  $\omega$  Cen are shown using the large filled triangles.

comparison Dorman et al., 1995 quote the metallicity of  $\omega$  Cen as -1.6 dex) and the best-fit age is  $15.08 \pm 0.4$  Gyr. We find that the discrepancy between the *FUV* luminosity-weighted age and the mass-weighted age of  $\omega$  Cen is  $\sim 3$  Gyr, which is very similar to what we found for the M87 GC population detected in the Sohn et al. (2006) study.

We collate all our findings in Figure 7. The filled circles show age and metallicity estimates for M87 GCs, derived using the  $\Delta Y/\Delta Z = 2$  model. Ages for M87 GCs, determined from the Lick indices, are overplotted using open triangles. The *FUV* luminosity-weighted (15.1 Gyr) and mass-weighted (12 Gyr) ages of  $\omega$  Cen are shown by the large filled triangles. The striking correspondence between the discrepancies in the luminosity and mass-weighted ages in both  $\omega$  Cen and the M87 GC population, indicates that a similar He enrichment to what is conjectured in  $\omega$  Cen would produce a similar enhancement of *FUV* flux in M87 GCs, causing their ages to be similarly overestimated by  $\sim 3$  Gyr.

## 5 SIMULATING THE M87 GC POPULATION

Figure 3 shows the observed  $UV$  GC data from M87 and the Milky Way. We find that even optically-red GCs show strong  $UV$  fluxes and blue  $UV - V$  colours ( $FUV - V \leq 2$ ). Sohn et al. (2006) found that all optically bright ( $V < 22$ ) GCs in M87 are also  $UV$  bright, regardless of their metallicities. Both in the Milky Way and M87 samples, there appears to be a positive and thus sensible correlation between  $V - I$  and  $FUV - V$ ; but the M87 GCs are brighter in the  $UV$  than their Milky Way counterparts by at least a magnitude or more. We note that, for a sample of M31 GCs detected in the  $FUV$  by the GALEX satellite mission, the same stellar models yield best-fit ages of 10-12 Gyr, using an identical parameter estimation technique (S. -C. Rey, private communication).

To investigate possible reasons for these surprising features of the M87 sample, we simulate a population of GCs using the GCLF and GC metallicity distribution function (MDF) in M87 (Figure 8), taken from Kundu et al. (1999). Each GC is allocated a formation age, drawn from a uniform distribution of values between 9 and 13 Gyr. This yields a synthetic population of GCs, each described by a  $V$ -band magnitude, a metallicity and a formation age. Using the fiducial stellar models ( $\Delta Y/\Delta Z = 2$ ), we then compute the apparent  $FUV$  magnitude of each GC, given its apparent  $V$ -band magnitude, metallicity and age. This results in the distribution of apparent  $FUV$  magnitudes shown in Figure 9. We now explore the characteristics of *GCs that we would expect to detect* in this simulated sample, given the  $FUV$  detection limit of 25 mag in the Sohn et al. (2006) study. Note that, although we have performed multiple ( $\sim 50,000$ ) simulations, the plots in this section describe results from a typical simulation of  $\sim 1000$  objects.

Based on a large number of simulations, we find that the *detectable* fraction of *normal* old GCs, is  $2.1 \pm 0.6$  percent. We note that this value is reasonably robust against the variation in the input distributions. Since the Sohn et al. (2006) study (excluding Field 4 because it has a lower detection limit and is not representative of the other fields) covers  $\sim 30$  percent of the WFPC2 image of Kundu et al. (1999), we would expect it to have  $\sim 300$  GCs in its field of view. In an ideal scenario, where *all* the detectable GCs are indeed picked up by the observations, a detection rate of  $\sim 2$  percent translates to  $\sim 6$  clusters detected in the  $FUV$ . The *actual* detection rate is *significantly higher*, with 66 sources detected by Sohn et al. (2006), of which 50 are confirmed as GCs through comparison with the Kundu et al. (1999) study. The number is lowered to 38 after cross-matching with Jordán et al. (2002). We

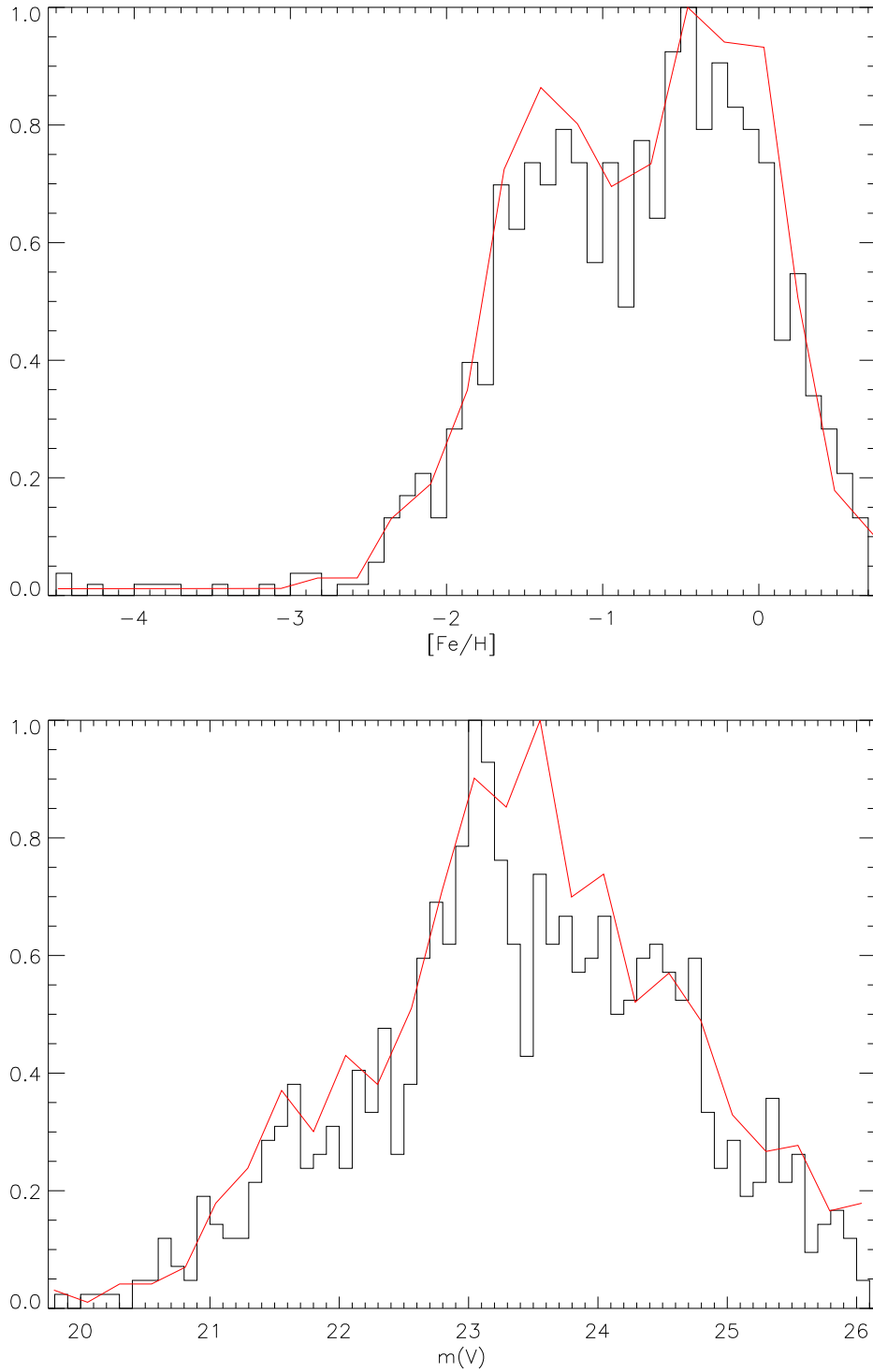


**Figure 8.** TOP: Simulated GC metallicities (histogram) and the metallicity distribution function from Kundu et al. (1999) (solid line). BOTTOM: Simulated GC V-band magnitudes (histogram) with the observed GCLF from Kundu et al. (1999) (solid line). The plots show a typical simulation of  $\sim 1000$  objects.

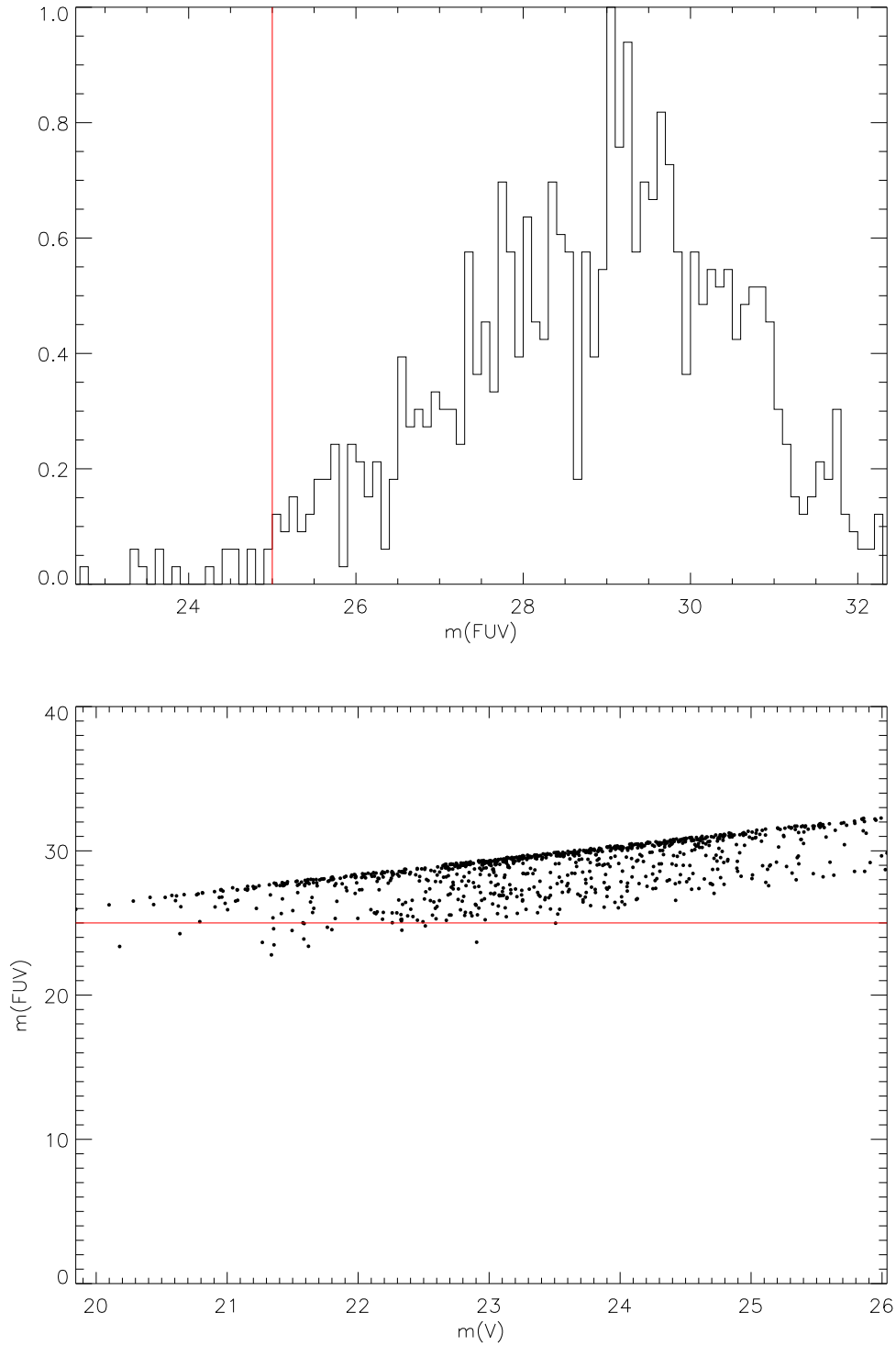


**Figure 9.** TOP: Simulated distribution of apparent GC  $FUV$  magnitudes. The solid line shows the detection limit of the Sohn et al. (2006) study. BOTTOM: Apparent  $FUV$  magnitudes vs. apparent  $V$ -band magnitudes for the simulated GCs. The solid line shows the detection limit of the Sohn et al. (2006) study. The plots show a typical simulation of  $\sim 1000$  objects.

therefore find that the detection rate achieved by this study is up to eight times higher than what might be expected on the basis of canonical stellar model predictions. Given the expected detection rate of  $\sim 2\%$ , the observed detection rate of  $\sim 17\%$  (50 out of 300) achieved by this study is a 24 sigma event!

We finish this section by comparing the *FUV* and optical colours of the observed sample to those in the simulations (Figure 10). As expected from the analysis presented in the preceding sections, we see a clear separation between the parameter space occupied by the simulated GCs and that occupied by the observed sample - we illustrate this using grids which plot the Sohn et al. (2006) *FUV* photometry against optical photometry from both Kundu et al. (1999) and Jordán et al. (2002).

## 6 SUMMARY AND DISCUSSION

We have studied the *UV* photometry from *HST/STIS* and optical photometry from *HST/WFPC2* photometry of 38 GCs in the Virgo elliptical M87. The dataset represents the best photometric GC dataset covering both the *UV* and the optical ranges. Parameter estimation of the age and metallicity of each M87 GC, using stellar models with standard He enrichment ( $\Delta Y/\Delta Z \sim 2$ ), results in almost all GCs having a best-fit age of 14–18 Gyr, significantly in excess of the currently accepted age of the Universe.

The metallicity estimation leads to an age distribution which shows no clear trend with metallicity at least in our limited sample. The marginalised metallicity PDF for the entire sample appears multi-modal. A KMM analysis for bimodality yields two peaks at -1.33 and -0.25 dex. These values agree (within errors) with previously determined values in Jordán et al. (2002) and Kundu et al. (1999). The significance of the agreement is however limited because our sample is a *FUV*-selected subset of the parent GC population and thus are affected by selection effects (and also low number statistics). The derived ages of the GCs in this study are significantly larger than the Lick-index-based ages of a more representative sample of the M87 *parent* GC population.

We have presented a *plausibility argument* that the ‘overestimate’ in the derived ages may be driven by enhanced *FUV* fluxes from anomalous HB components in these GCs, similar to those postulated by Lee et al. (2005) in the Galactic GC  $\omega$  Cen, where a sub-population of EHB stars, which are hotter and super-helium-enriched compared to the primary population of normal HB stars, enhance the overall *FUV* flux more than would be normally expected.

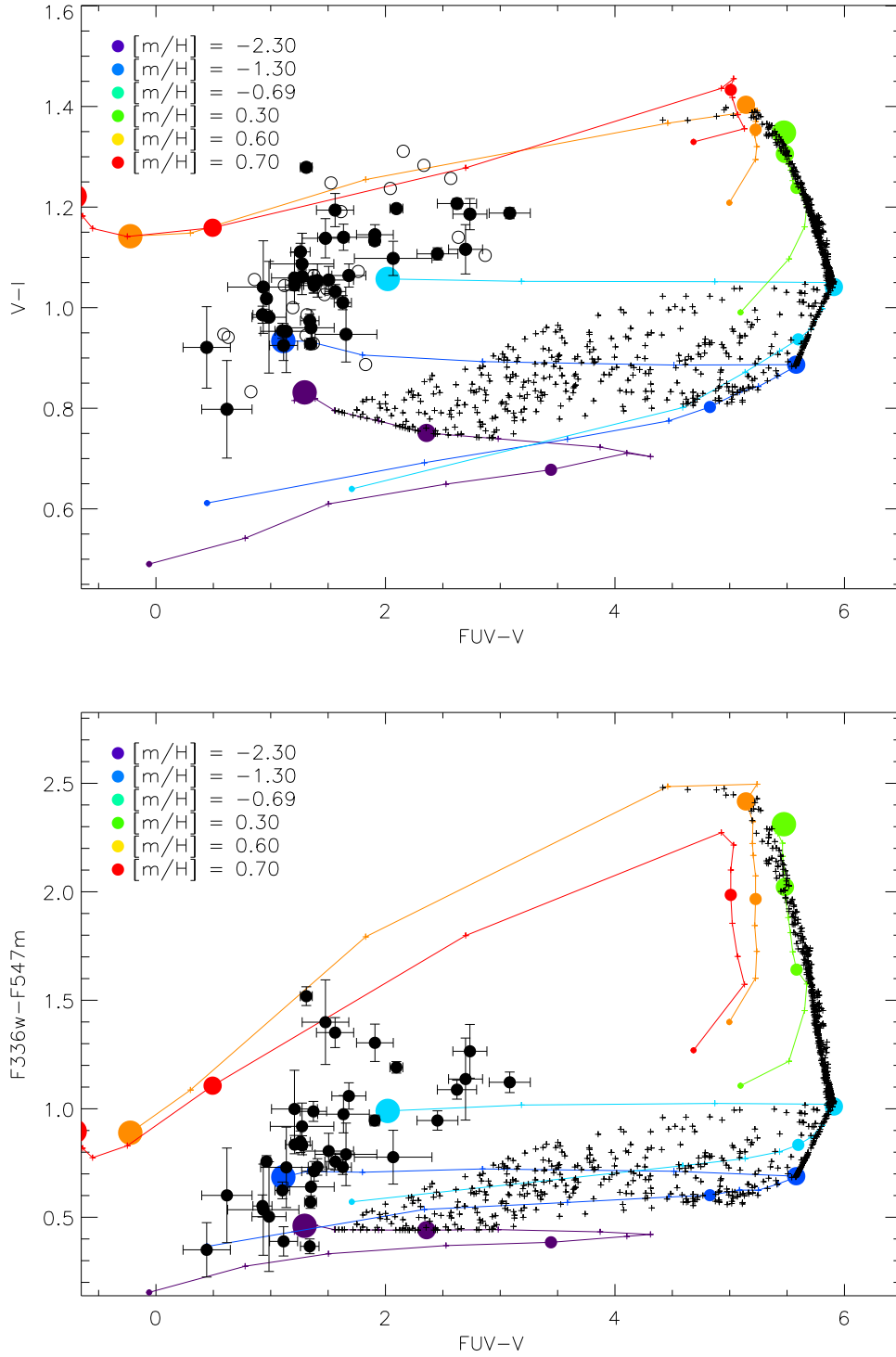


**Figure 10.** TOP:  $(FUV - V)$  vs.  $(V - I)$  for observed (filled circles with error bars) and simulated GCs (crosses) plotted on top of a model grid generated from stellar models with the fiducial value of He enrichment ( $\Delta Y/\Delta Z = 2$ ). Filled circles represent the 38 GCs used in this study after cross-matching the Sohn et al. (2006) catalog with that of both Jordán et al. (2002) and Kundu et al. (1999). We also indicate, using open circles, GCs which appear in Sohn et al. (2006) and Kundu et al. (1999) but not in Jordán et al. (2002), and which are therefore excluded from the parameter estimation. The lowest model age plotted is 1 Gyr and the largest age plotted is 15 Gyr. Ages 1, 5, 10 and 15 Gyr are shown using filled circles of increasing sizes. BOTTOM:  $(FUV - V)$  vs.  $(F336w - F547m)$  for observed (filled circles with error bars) and simulated GCs (crosses), plotted on top of a model grid generated from stellar models with the fiducial value of He enrichment ( $\Delta Y/\Delta Z = 2$ ).



To support this hypothesis, we have first shown that replacing the fiducial stellar model, which assumes  $\Delta Y/\Delta Z = 2$ , with a modestly helium-enhanced stellar model ( $\Delta Y/\Delta Z = 3$ ) lowers the best-fit ages of only the *metal-rich* M87 GCs by  $\sim 1$  to 2 Gyr. We have then compared the *FUV* luminosity-weighted age of  $\omega$  Cen, derived from its *UV* photometry in Dorman et al. (1995), to its ‘true’ age, calculated from the mass-weighted mean age of the best-fit  $\omega$  Cen model of Lee et al. (2005). We have found that this “true” age is around 12 Gyr compared to a *FUV* luminosity-weighted age of around 15.1 Gyr - a discrepancy of 3 Gyr, which is very similar to the case of the *FUV* bright M87 GCs in our sample.

Given the striking similarity in the discrepancy between the *FUV* luminosity-weighted and mass-weighted ages of both  $\omega$  Cen and M87 GCs, we suggest that a similar type of extreme He enrichment scenario could, in principle, produce the enhanced EHB components in the M87 GCs. Given the fact that our M87 sample is *FUV* selected, it is not surprising that we detect mainly those GCs which show enhanced EHB components (and therefore enhanced *FUV* fluxes), leading to overestimates of their ages when stellar models with fiducial values of primordial He abundance are applied. This hypothesis is supported by a simulation of M87 GCs, which indicates that the detection rate for old GCs, given the GCLF, GC MDF, area covered by the Sohn et al. (2006) study, and assuming formation ages between 9 and 13 Gyr, should only be around 2 percent - the actual detection rate is up to eight times higher. Since few GCs are expected to be observed but a significant number *are* detected, it is natural to conclude that the *FUV* fluxes are enhanced in the majority of the detected GCs. Although we cannot prove its validity based on this argument, the super-He-rich hypothesis offers a reasonable explanation.

It is clear that drawing conclusions about the *global FUV* properties of the M87 GC population, based on this “super-helium-enriched” subsample alone, is not practical. Deeper observations are required to sample both more GCs with enhanced EHB components and also normal GCs which conform to the expectations of the stellar models for old populations (such as those found in M31). The presence of super-He-rich stellar populations in Galactic GCs such as  $\omega$  Cen and in the M87 GC systems raises the intriguing possibility that this phenomenon may be present, in varying degrees, in most systems in the nearby Universe. A good example of such a case could be the UV upturn phenomenon of elliptical galaxies (Code & Welch 1979; Burstein et al. 1988; O’Connell 1999). Indeed, this study may be the first to discover signatures of apparent He enrichment in extragalactic objects. Future *UV* surveys of nearby GC systems are therefore highly anticipated, both to establish the possible

ubiquity of the He enrichment phenomenon and to measure the degree to which stellar populations may be He enriched.

## ACKNOWLEDGMENTS

We warmly thank Andres Jórđan for providing HST WFPC2 data on the M87 globular clusters and for numerous comments, without which this paper would not have been possible. He was involved in this work from the beginning but declined our offer of the much-deserved co-authorship following his work ethics, which we admire. We also thank the anonymous referee for encouragements and clarifications. This work was supported by grant No. R01-2006-000-10716-0 from the Basic Research Program of the Korea Science & Engineering Foundation and Yonsei University Research Fund to S.K.Y.

## REFERENCES

- Bedin L. R., Piotto G., Anderson J., Cassisi S., King I. R., Momany Y., Carraro G., 2004, *ApJ*, 605, L125
- Bedin L. R., Piotto G., Zoccali M., Stetson P. B., Saviane I., Cassisi S., Bono G., 2000, *A&A*, 363, 159
- Bekki K., Norris J. E., 2006, *ApJ*, 637, L109
- Bruzual G., Charlot S., 2003, *MNRAS*, 344, 1000
- Burstein D., Bertola F., Buson L. M., Faber S. M., Lauer T. R., 1988, *ApJ*, 328, 440
- Caloi V., & D'Antona F., 2006, *A&A* in press, Astro-ph/0610406
- Choi E., & Yi S. K., 2007, *MN*, 375, 1
- Code A. D., Welch G. A., 1979, *ApJ*, 228, 95
- Cohen J. G., Blakeslee J. P., Ryzhov A., 1998, *ApJ*, 496, 808
- D'Antona F., Bellazzini M., Caloi V., Pecci F. F., Galletti S., Rood R. T., 2005, *ApJ*, 631, 868
- D'Antona F., & Caloi V., 2004, *ApJ*, 611, 871
- Dorman B., O'Connell R. W., Rood R. T., 1995, *ApJ*, 442, 105
- Ferraro F. R., Sollima A., Pancino E., Bellazzini M., Straniero O., Origlia L., Cool A. M., 2004, *ApJ*, 603, L81
- Jordán A., Côté P., West M. J., Marzke R. O., 2002, *ApJ*, 576, L113
- Karakas A., Fenner Y., Sills A., Campbell S. & Latanzio J., *ApJ*, in press; Astro-ph/0608366

- Kundu A., Whitmore B. C., Sparks W. B., Macchetto F. D., Zepf S. E., Ashman K. M., 1999, *ApJ*, 513, 733
- Lee H.-c., Yoon S.-J., Lee Y.-W., 2000, *AJ*, 120, 998
- Lee Y.-W., Joo S.-J., Han S.-I., Chung C., Ree C. H., Sohn Y.-J., Kim Y.-C., Yoon S.-J., Yi S. K., Demarque P., 2005, *ApJ*, 621, L57
- Norris J. E., 2004, *ApJ*, 612, L25
- O'Connell R. W., 1999, *ARAA*, 37, 603
- Peimbert M., Carigi L., Peimbert A., 2001, *ApSSS*, 277, 147
- Piotto G., Villanova S., Bedin L. R., Gratton R., Cassisi S., Momany Y., Recio-Blanco A., Lucatello S., Anderson J., King I. R., Pietrinferni A., Carraro G., 2005, *ApJ*, 621, 777
- Sohn S. T., O'Connell R. W., Kundu A., Landsman W. B., Burstein D., Bohlin R. C., Frogel J. A., Rose J. A., 2006, *AJ*, 131, 866
- Sollima A., Borissova J., Catelan M., Smith H., Minniti D., Cacciari C., Ferraro F. R., 2006, *ApJ*, p. in press
- Sollima A., Ferraro F. R., Pancino E., Bellazzini M., 2005, *MNRAS*, 357, 265
- Spergel D. et al. 2006, *ApJ*, submitted; Astro-ph/0603449
- Sweigart A., & Catelan M. 1998, *ApJ*, 501, L63
- Whitney J. H., O'Connell R. W., Rood R. T., Dorman B., Landsman W. B., Cheng K.-P., Bohlin R. C., Hintzen P. M. N., Roberts M. S., Smith A. M., Smith E. P., Stecher T. P., 1994, *AJ*, 108, 1350
- Worthey G., 1994, *ApJS*, 95, 107
- Yi S., Demarque P., Oemler A., 1997, *ApJ*, 486, 201
- Yi S., Demarque P., Oemler A., 1998, *ApJ*, 492, 480
- Yi S., Lee, Y.-W., Woo, J.-H., Park, J.-H., Demarque P., & Oemler A., 1999, *ApJ*, 492, 480
- Yi S. K., 2003, *ApJ*, 582, 202